

# Higher order cumulants of electric charge and strangeness fluctuations on the crossover line

J. Goswami<sup>1</sup>, F. Karsch<sup>1</sup>, S. Mukherjee<sup>2</sup>, C. Schmidt<sup>1</sup> and D. Bollweg<sup>1</sup>  
HotQCD Collaboration

<sup>1</sup>Bielefeld University, <sup>2</sup>Brookhaven National Lab

Criticality in QCD and the Hadron Resonance Gas, Wroclaw | 30.07.2020

- 1 QCD Phase Diagram
- 2 Fluctuations via lattice QCD
- 3 Electric charge fluctuations
- 4 Strangeness fluctuations

- ▶ Smooth crossover for  $\mu_B < 300$  MeV.
- ▶ Recent result from lattice QCD [arXiv:1812.08235]:

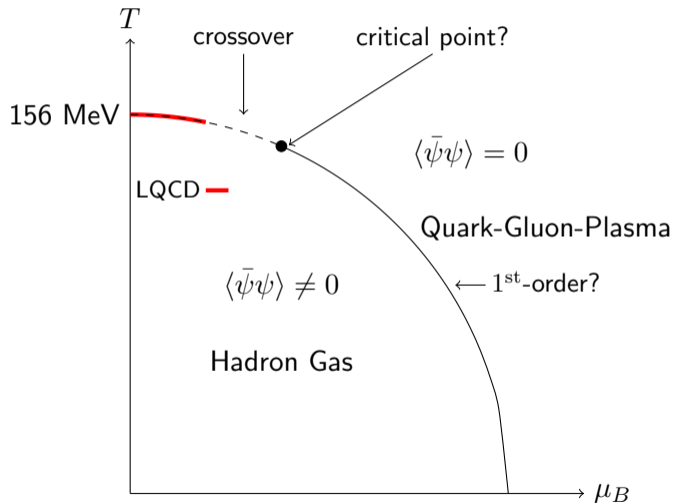
$$T_{pc}(\mu_B) = T_{pc,0} \left( 1 - \kappa_2^{B,f} \bar{\mu}_B^2 - \kappa_4^{B,f} \bar{\mu}_B^4 \right)$$

with  $\bar{\mu}_B = \frac{\mu_B}{T_{pc,0}}$ ,  $T_{pc,0} = 156.5 \pm 1.5$  MeV,

$$\kappa_2^{B,f} = 0.012 \pm 0.004,$$

$$\kappa_4^{B,f} = 0.000 \pm 0.004$$

- ▶ Rest of the phase diagram largely unknown.



- ▶ Chiral crossover overlaps with chemical freeze-out in heavy ion collisions:  $T_{cf}(\mu_B \sim 0) = 156.5$  MeV [Andronic et al. Nature 2018].
- ▶ Transition region is accessible through HIC experiments.
- ▶ Cumulants of conserved charge fluctuations are ideal probes to study phase diagram: maxima along crossover line, divergence at CEP.

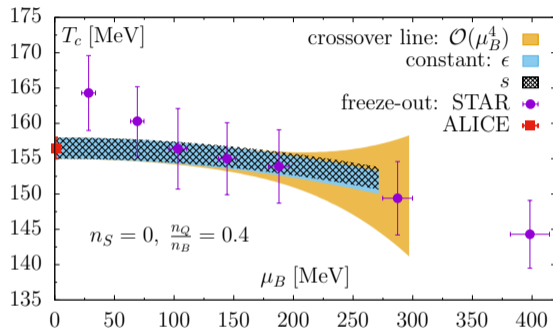


Figure: Freeze-out vs. chiral transition temperature from HotQCD [arXiv:1812.08235].

**Goal: first-principle QCD predictions for cumulant ratios  $M/\sigma^2, S\sigma, \kappa\sigma^2, \dots$  etc.**

$M/\sigma^2, S\sigma, \kappa\sigma^2$  are accessible via *generalized susceptibilities*  $\chi$ :

$$\chi_{ijk}^{BQS} \equiv \frac{1}{VT^3} \frac{\partial^{i+j+k} \log \mathcal{Z}}{\partial \hat{\mu}_B^i \partial \hat{\mu}_Q^j \partial \hat{\mu}_S^k}, \quad \hat{\mu}_X \equiv \frac{\mu_X}{T}$$

$$M_X/\sigma_X^2 = \frac{\chi_1^X}{\chi_2^X}, \quad S_X\sigma_X = \frac{\chi_3^X}{\chi_2^X}, \quad \kappa_X\sigma_X^2 = \frac{\chi_4^X}{\chi_2^X} \quad \text{with } X = B, Q, S$$

- ▶ Finite-density sign problem renders direct simulations at  $\mu_B > 0$  impossible.
- ▶ Use constrained Taylor-Expansion in  $\mu$  to access cumulants at finite density.
- ▶ Impose strangeness neutrality  $n_S = 0$  and  $\frac{n_Q}{n_B} = 0.4$  order by order - corresponds to thermal conditions in HIC (e.g. Pb + Pb or Au + Au).

- ▶ Dynamical Fermions (HISQ) with  $N_f = 2 + 1$ : two light Quarks (up + down) and a strange Quark with mass ratio  $\frac{m_s}{m_l} = 27$ .  $\Rightarrow$  physical meson masses in the continuum limit!
- ▶ Lattice sizes  $32^3 \times 8$ ,  $48^3 \times 12$  and  $64^3 \times 16$  at 9 different temperatures each.
- ▶ Large simulation campaign on Summit in 2019 & 2020: Compared to our earlier analysis of baryon skewness and kurtosis [arXiv:1708.04897v3] we increased statistics in the vicinity of  $T_{pc}$  on  $N_t = 8$  lattices by a factor 3-4 and on  $N_t = 12$  lattices by a factor 6-8.

	$N_t = 8$	$N_t = 12$	$N_t = 16$
No. of Conf.	$1.2 \cdot 10^6$	$2 - 4 \cdot 10^5$	$10^4$

- ▶ High statistics data enable us to calculate cumulants up to N<sup>3</sup>LO in  $\mu_B$  (previous studies: NLO).
- ▶ **All data on fluctuations in this presentation are HotQCD preliminary.**

- ▶ Cumulant ratios are scanned in  $\mu_B$

$$R_{nm}^X(T, \mu_B) = \frac{\sum_i \frac{1}{i!} \chi_n^{X,i} \left(\frac{\mu_B}{T}\right)^i}{\sum_j \frac{1}{j!} \chi_m^{X,j} \left(\frac{\mu_B}{T}\right)^j}$$

- ▶ Results like Fig. 2 for each  $N_t$  are jointly fitted assuming  $1/N_t^2$  corrections  $\rightarrow$  continuum extrapolation.
- ▶ The fitted surface can then be evaluated along arbitrary lines in  $(T, \mu_B)$  if desired. In the following:  $T_{pc}(\mu_B)$

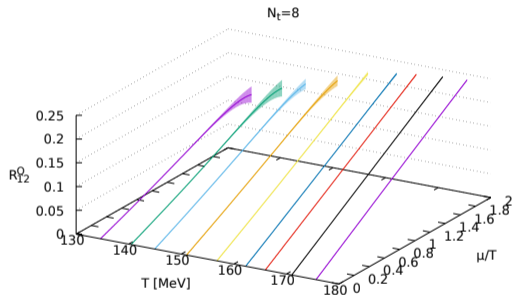


Figure:  $R_{12}^Q$  for  $N_t = 8$  scanned in  $\mu_B/T$ .

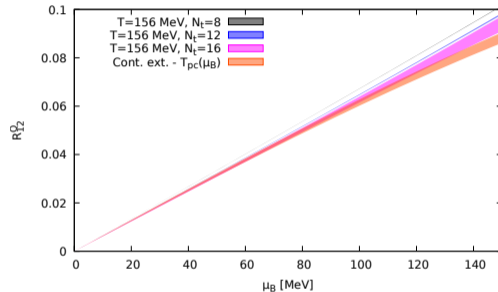
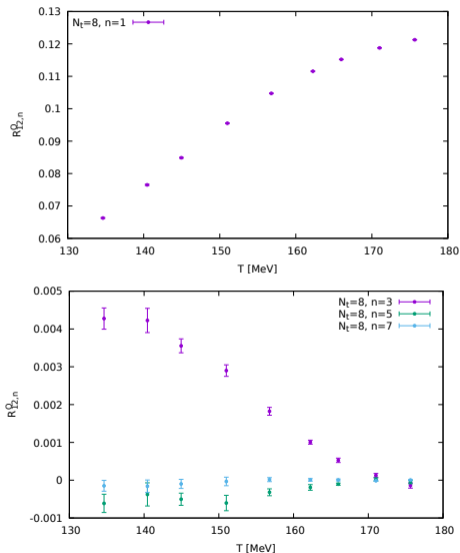


Figure: Left: Contributions to  $R_{12}^Q$  sorted by order in  $\mu_B$ . Right:  $R_{12}^Q$  along  $T_{pc}(\mu_B)$ .



- ▶  $R_{12}^Q$  dominated by leading order contribution  $\sim \mu_B$ .
- ▶ NLO contributions smaller by an order of magnitude.
- ▶ Mild temperature dependence.
- ▶ Ideal for extracting freeze-out chemical potential  $\mu_{B,f} \Rightarrow$  "Baryometer"

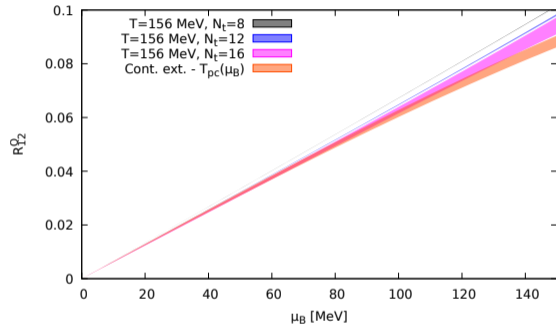


Figure:  $R_{12}^Q$  for different  $N_t$  and continuum extrapolation along  $T_{pc}(\mu_B)$ .

Freeze-out chemical potential extracted by comparing to data from STAR<sup>1</sup>:

$\sqrt{s_{NN}}$ [GeV]	$\mu_{B,f}$ [MeV]
200	19.4(1)
62.4	58(1)
39	92(2)
27	131(3)

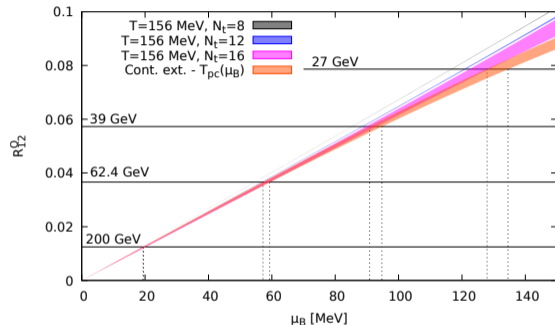


Figure:  $R_{12}^Q$  for different  $N_t$  and continuum extrapolation along  $T_{pc}(\mu_B)$ .

<sup>1</sup>[PRL 113, 092301 (2014)]

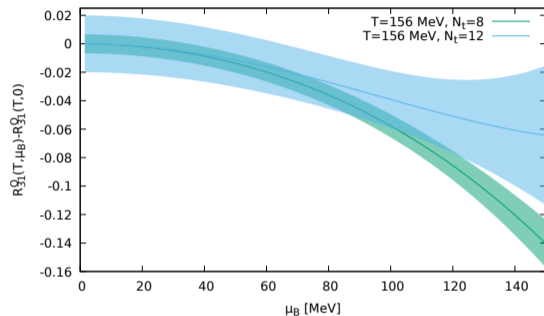
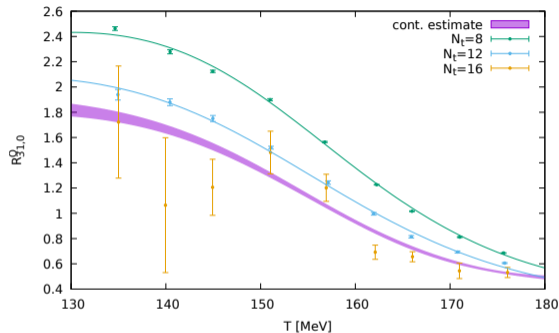


Figure: Left:  $R_{31}^Q$  at  $\mu_B = 0$ . Right:  $\mu_B$  dependence around  $T_{pc}$ .

- ▶ Strong temperature dependence/ weak  $\mu_B$  dependence  $\Rightarrow$  "Thermometer"

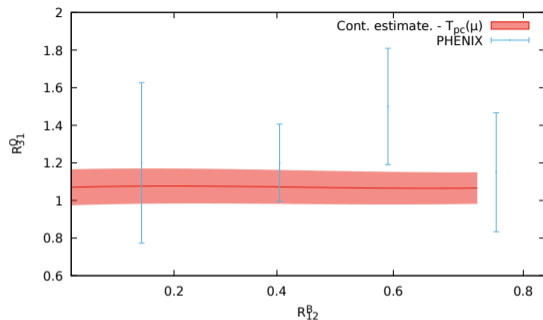
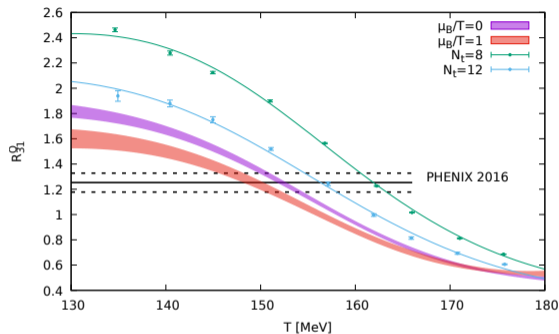


Figure: Cont. estimate of  $R_{31}^Q(T_{pc}(\mu_B))$ .

- ▶ Lattice QCD estimate:  $R_{31}^Q(T_{pc}(\mu_B)) = 1.07(9)$ .
- ▶ PHENIX<sup>1</sup> Measurements of  $R_{31}^Q$  consistent with freeze-out at  $T_{pc}$ .
- ▶ Note: published PHENIX data use  $N_T = 8$  lattice results  $\rightarrow$  too high  $T_f$ .

<sup>1</sup>[Phys. Rev. C 93, 011901(R) (2016)]

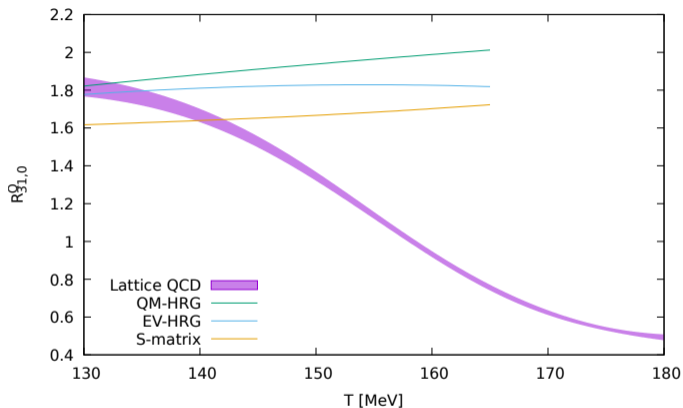


Figure:  $R_{31}^Q$  via lattice QCD vs. different HRG calculations.

- ▶  $R_{31}^Q$  shows large deviations from HRG in the transition region.
- ▶ T-dependence of  $R_{31}^Q(T, \mu_B = 0)$  is not captured by any of the non-interacting HRG models

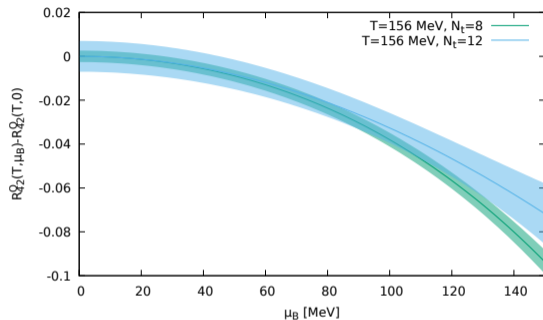
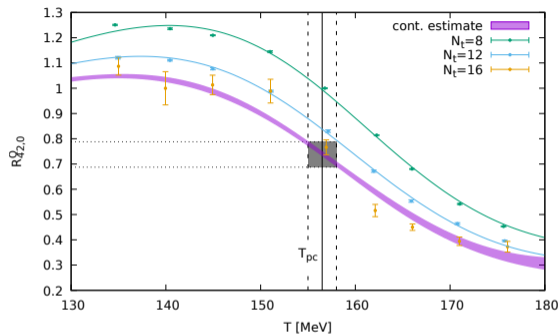


Figure: Left:  $R_{42}^Q$  at  $\mu_B = 0$ . Right:  $\mu_B$  dependence around  $T_{pc}$ .

- ▶ Significantly smaller errors compared to  $R_{31}^Q$  since noisy baryon correlations do not contribute to LO. LQCD Estimate:  $R_{42}^Q(T_{pc}, 0) = 0.73(5)$ .
- ▶ Avg. over PHENIX data:  $R_{42}^Q = 1.29(6)$  inconsistent with lattice results.

- ▶ Constraint  $n_S(\mu_B, \mu_S) \stackrel{!}{=} 0$  determines  $\mu_S$ :

$$\frac{\mu_S}{\mu_B} = s_1(T) + s_3(T) \left(\frac{\mu_B}{T}\right)^2 + \mathcal{O}\left(\left(\frac{\mu_B}{T}\right)^4\right).$$

- ▶  $s_n(T)$ : Consists of combinations of  $\chi_{ijk}^{BQS}$  directly accessible in LQCD.
- ▶ Main contribution to  $s_1(T)$  comes from  $\frac{\chi_{11}^{BS}}{\chi_2^S}$ .
- ▶  $s_n$  with  $n \geq 3$  almost negligible.
- ▶ QCD result on  $\mu_S/\mu_B$  sensitive to strangeness content (in a HRG model).
- ▶ Excellent match with QM-HRG.

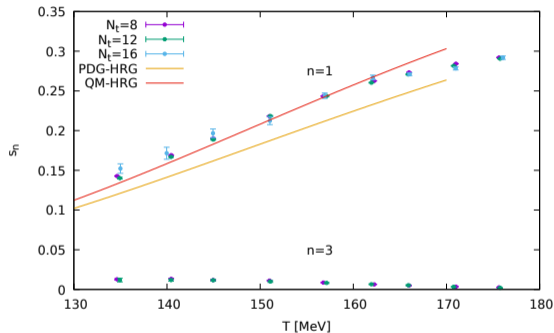


Figure:  $s_1(T)$  and  $s_3(T)$  from lattice QCD and HRG.

## Lattice QCD:

- ▶ Constraint  $n_S(\mu_B, \mu_S) \stackrel{!}{=} 0$  determines  $\mu_S$ :

$$\frac{\mu_S}{\mu_B} = s_1(T) + s_3(T) \left( \frac{\mu_B}{T} \right)^2 + \mathcal{O} \left( \left( \frac{\mu_B}{T} \right)^4 \right).$$

- ▶  $s_n(T)$ : Consists of combinations of  $\chi_{ijk}^{BQS}$  directly accessible in LQCD.
- ▶ Main contribution to  $s_1(T)$  comes from  $\frac{\chi_{11}^{BS}}{\chi_2^S}$ .
- ▶  $s_n$  with  $n \geq 3$  almost negligible.
- ▶ QCD result on  $\mu_S/\mu_B$  sensitive to strangeness content (in a HRG model).
- ▶ Excellent match with QM-HRG.

## Heavy Ion Collisions:

- ▶ HRG relation for  $\bar{B}$  to  $B$  yields can be used:

$$\frac{\bar{B}}{B}(\sqrt{s}) = \exp \left( -\frac{\mu_B}{T} (2 - 2|S| \frac{\mu_S}{\mu_B}) \right)$$

- ▶  $\frac{\mu_S}{\mu_B}$  obtainable by fitting yields for different particle species in  $|S|$ .



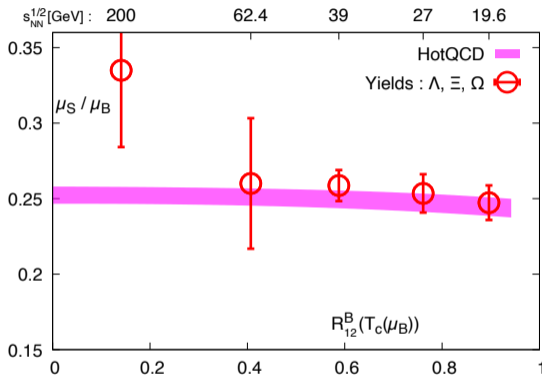


Figure:  $\mu_S/\mu_B$  along  $T_{pc}(\mu_B)$  vs.  $\mu_S/\mu_B$  extracted from STAR<sup>1</sup>

►  $\mu_{S,f}/\mu_{B,f}$  from strange baryon yields is consistent with lattice QCD results at  $T_{pc}$ !

<sup>1</sup>arXiv:1010.0142 & arXiv:1906.03732

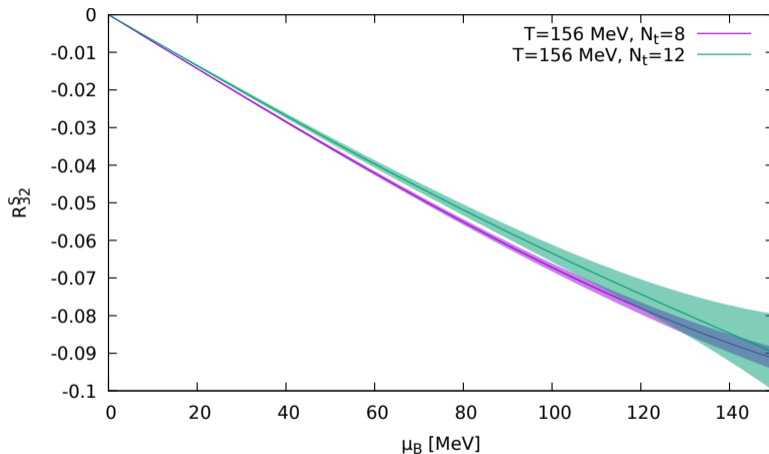


Figure:  $R_{32}^S(T_{pc}, \mu_B)$  for  $N_t = 8, 12$  lattices.

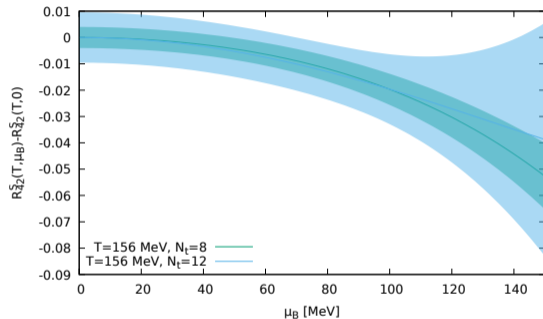
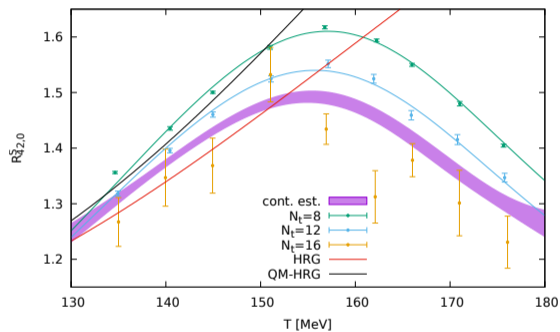


Figure: Left:  $R_{42}^S$  at  $\mu_B = 0$ . Right:  $\mu_B$ -dependence around  $T_{pc}$ .

- ▶ Precise calculations of  $R_{12}^Q(T_{pc}(\mu_B))$  to NNNLO in  $\mu_B$  enabled determination of  $\mu_{B,f}$  from Event-by-Event fluctuation data by STAR.
- ▶ PHENIX data on  $R_{31}^Q$  are consistent with  $T_f \sim T_{pc}$  when comparing to NNLO lattice QCD continuum estimates.
- ▶ Non-interacting HRG models are not suitable to describe thermodynamics of higher order electric charge fluctuations.
- ▶  $\mu_S/\mu_B$  lattice QCD results are well described by QM-HRG which justifies extraction of  $\mu_{S,f}$  from experimentally measured strange baryon yields.
- ▶ Apart from  $R_{42}^Q$ , electric charge and strangeness results are consistent with freeze-out at  $T_{pc}(\mu_B)$ .